Regulation of a viral proteinase by a peptide and DNA in one-dimensional space. I. binding to DNA and to hexon of the precursor to protein VI, pVI, of human adenovirus

Graziano, Vito ; McGrath, William J ; Suomalainen, Maarit ; Greber, Urs F ; Freimuth, Paul ; Blainey, Paul C ; Luo, Guobin ; Xie, X Sunney ; Mangel, Walter F

Abstract: The precursor to adenovirus protein VI, pVI, is a multifunctional protein with different roles early and late in virus infection. Here we focus on two roles late in infection, binding of pVI to DNA and to the major capsid protein hexon. pVI bound to DNA as a monomer independent of DNA sequence with an apparent equilibrium dissociation constant, K(d(app.)), of 46 nM. Bound to double-stranded DNA, one molecule of pVI occluded 8 base pairs. Upon the binding of pVI to DNA, 3 sodium ions were displaced from the DNA. A ΔG of -4.54 kcal/mol for the nonelectrostatic free energy of binding indicated that a substantial component of the binding free energy resulted from nonspecific interactions between pVI and DNA. The proteolytically processed, mature form of pVI, protein VI, also bound to DNA; its K(d(app.)) was much higher, 307 nM. The binding assays were performed in 1 mM MgCl(2), because in the absence of magnesium, the binding to pVI or protein VI to DNA was too tight to determine a K(d(app.)). Three molecules of pVI bound to one molecule of the hexon trimer with an equilibrium dissociation constant K(d(app.)) of 1.1nM.

DOI: https://doi.org/10.1074/jbc.M112.377150

THE JOURNAL OF BIOLOGICAL CHEMISTRY VOL. 288, NO. 3, pp. 2059–2067, January 18, 2013
Published in the U.S.A.

Regulation of a Viral Proteinase by a Peptide and DNA in One-dimensional Space

*I. BINDING TO DNA AND TO HEXON OF THE PRECURSOR TO PROTEIN VI, pVI, OF HUMAN ADENOVIRUS**

Received for publication, April 30, 2012, and in revised form, August 2, 2012 Published, JBC Papers in Press, October 7, 2012, DOI 10.1074/jbc.M112.377150

Vito Graziano[‡], William J. McGrath[‡], Maarit Suomalainen[§], Urs F. Greber[§], Paul Freimuth[‡], Paul C. Blainey[¶1], Guobin Luo[¶], X. Sunney Xie[¶2], and Walter F. Mangel[‡3]

From the [‡]Biology Department, Brookhaven National Laboratory, Upton, New York 11973, the [§]Institute of Molecular Life Sciences, University of Zurich, Winterthurerstrasse 190, CH-8057 Zurich, Switzerland, and the [¶]Department of Chemistry and Chemical Biology, Harvard University, Cambridge, Massachusetts 02138

Background: The C terminus of pVI activates the adenovirus proteinase. pVI escorts hexon into the nucleus.
Results: pVI binds tightly to DNA independent of sequence, K_d = 46 nM. pVI binds tightly to hexon, K_d = 1.1 nM.
Conclusion: DNA binding of pVI is the first step in the activation of adenovirus proteinase.
Significance: This step links pVI, hexon, viral DNA, and the adenovirus proteinase in virion maturation.

The precursor to adenovirus protein VI, pVI, is a multifunctional protein with different roles early and late in virus infection. Here, we focus on two roles late in infection, binding of pVI to DNA and to the major capsid protein hexon. pVI bound to DNA as a monomer independent of DNA sequence with an apparent equilibrium dissociation constant, $K_{d(app)}$, of 46 nM. Bound to double-stranded DNA, one molecule of pVI occluded 8 bp. Upon the binding of pVI to DNA, three sodium ions were displaced from the DNA. A ΔG^0_0 of −4.54 kcal/mol for the nonelectrostatic free energy of binding indicated that a substantial component of the binding free energy resulted from nonspecific interactions between pVI and DNA. The proteolytically processed, mature form of pVI, protein VI, also bound to DNA; its $K_{d(app)}$ was much higher, 307 nM. The binding assays were performed in 1 mM $MgCl_2$ because in the absence of magnesium, the binding to pVI or protein VI to DNA was too tight to determine a $K_{d(app)}$. Three molecules of pVI bound to one molecule of the hexon trimer with an equilibrium dissociation constant $K_{d(app)}$ of 1.1 nM.

Many viral proteins contain several different domains that function at different steps during a virus infection. This is certainly true of the precursor to protein VI, pVI,[4] and of its proteolytically processed product, protein VI, of adenovirus that are involved in steps both early and late in infection. Early in infection, virus particles engage in a stepwise disassembly program coordinated in time and space during entry into cells leading to the delivery of the viral genome into the nucleus for replication (1–4). Protein VI is involved in endosome disruption (5, 6). Late in infection, new virus particles are assembled and rendered infectious. pVI interacts with DNA to activate the adenovirus proteinase (AVP) (41) and with hexon, the major structural proteins of adenovirus, to escort hexon into the nucleus (7, 8).

Adenoviruses (9) are nonenveloped, icosahedral eukaryotic viruses that infect a wide range of species. In the subgroup C of human adenoviruses, Ad2 or Ad5 are the best characterized. They have an ~36-kb double-stranded DNA genome (10). The Ad2/Ad5 particle is about 90 nm in diameter and consists of an outer capsid surrounding an inner nucleoprotein core. Hexon, penton base, and fiber are the major structural proteins in the outer capsid. Hexon is the major protein of the facets of the icosahedral virus. The size of the hexon molecule can vary with the serotype; the largest, from Ad2, has 967 amino acids (9). There are 720 copies of hexon present as 240 homotrimers per virion. One face of the hexon trimer in the capsid is exposed to the core of the virus and hence the viral DNA. Protein VI is thought to lie within the internal cavity of each hexon trimer (11–16). There are 360 copies of protein VI, which contains 206 amino acids. Protein VI has been shown to bind to DNA independent of nucleotide sequence (17).

Initiation of an Ad2/Ad5 infection occurs when the capsid binds to high affinity receptors on the cell surface (3, 18–20), and the virus particle is internalized via clathrin-mediated endocytosis (21–23). After internalization, protein VI, the proteolytically processed form of pVI, is rapidly exposed (3, 24).

* This work was supported, in whole or in part, by the National Institutes of Health Director's Pioneer Award and the National Science Foundation (to X. S. X.) and National Institutes of Health R01AI41599 Grant (to W. F. M.). This work was also supported by the Swiss National Science Foundation (Grant 31003A_125477/1) and the Kanton Zurich (to U. F. G.) and by a Laboratory Directed Research and Development grant from Brookhaven National Laboratory (to P. C. F.).

[1] Present address: Broad Institute, Massachusetts Institute of Technology, 7 Cambridge Center, Cambridge MA, 02142.
[2] To whom correspondence may be addressed: Dept. of Chemistry and Chemical Biology, Harvard University, 12 Oxford St., Cambridge, MA 02138. Tel.: 617-496-9925; Fax: 617-496-8709; E-mail: xie@chemistry.harvard.edu.
[3] To whom correspondence may be addressed: Biology Dept., Brookhaven National Laboratory, 50 Bell Ave., Upton, NY 11973. Tel.: 631-344-3373; Fax: 631-344-3407; E-mail: mangel@bnl.gov.

[4] The abbreviations used are: pVI, the precursor to adenovirus protein VI; Ad2, human adenovirus serotype 2; Ad5, human adenovirus serotype 5; AVP, adenovirus proteinase; DDM, *n*-dodecyl-β-D-maltopyranoside; K_d(app), apparent equilibrium dissociation constant; Bis-Tris-propane, 1,3-bis[tris(hydroxymethyl)methylamino]propane; Cbz, carboxybenzyl.

Protein VI mediates endosome disruption, so the partially uncoated capsid can enter the cytoplasm (5).

Late in adenovirus infection, the genes for pVI, AVP, and hexon are transcribed from the L3 transcription region on the viral DNA (25). AVP is synthesized as an inactive enzyme (26, 27). The nuclear transport of hexon is mediated by pVI as hexon does not have a nuclear localization signal. pVI contains two nuclear export signals and two nuclear localization signals (7, 28, 29). pVIc,[5] the last 11 amino acids of pVI, contains an nuclear localization signal. It has been shown that the nuclear import of hexon in cultured cells occurs via pVI, which shuttles between the nucleus and the cytoplasm and appears to provide an adaptor for hexon import (7).

Adenovirus virions are assembled in part from precursor proteins. Of the 12 major virion proteins, six are precursor proteins in the young virion, an assembly intermediate. The penultimate step before the appearance of infectious virus is the activation of the AVP, a 23-kDa cysteine proteinase (30, 31) followed by the processing of the virion precursor proteins. AVP is activated by two cofactors, pVIc (GVQSLKRRRCF) (26, 27), the 11-amino acid peptide from the C terminus of pVI (26). In pVI, an AVP consensus cleavage site, IVGL ↓ G, immediately precedes pVIc and is cleaved by AVP between Leu and Gly to release pVIc (41). The other cofactor, the viral DNA genome (26, 32, 33), consists of 35,937 bp of linear DNA in the case of Ad2. The viral cofactors dramatically stimulate the macroscopic kinetic constants for substrate hydrolysis (32, 34, 35). The relative k_{cat}/K_m of AVP is enhanced 110-fold in the presence of DNA and 1130-fold in the presence of pVIc. When both cofactors are bound to AVP, the k_{cat}/K_m increases synergistically, by 16,000-fold. AVP, pVI, pVIc, and AVP-pVIc complexes (where AVP-pVIc is a noncovalent or covalently linked heterodimer of AVP and pVIc) bind tightly to DNA with nanomolar equilibrium dissociation constants; binding is independent of nucleic acid sequence (see Table 1) (26, 32, 33, 36, 41).

How does pVI activate AVP, and in particular, is DNA involved in that process? If so, what is the nature of its role? Here, we clone and express the genes for pVI and its mature, processed form, protein VI, purifying both proteins from *Escherichia coli*. We show that pVI does indeed bind to DNA independent of DNA sequence. We quantitatively characterize that interaction, and, in the next paper in this series (41), we show that novel modes of interaction with DNA are crucial to the activation of AVP by pVI. Here, we also characterize, quantitatively, the interaction of pVI and hexon, providing a molecular basis for the previously observed pVI dependence of hexon import to the nucleus (7).

EXPERIMENTAL PROCEDURES

Materials—The 11-amino acid peptide pVIc (GVQSLKRRRCF) was purchased from New England Peptide Inc. (Gardner, MA). The 5′-fluorescein-labeled 33-mer DNA, 36-mer DNA, 60-mer DNA, and the strands complementary to these DNAs were purchased from Invitrogen, as was streptavidin Alexa Fluor 546. Annealing of complementary DNAs was done as described previously (35). The 1500-mer dsDNA was obtained by sonicating *Cupriavidus metallidurans* CH_{34} genomic DNA. *n*-Dodecyl-β-D-maltopyranoside (DDM) was purchased from Anatrace (Maumee, OH). Cy3B monomaleimide was purchased from GE Healthcare. 5-Iodoacetamidofluorescein was purchased from Pierce. The complex (pVIc-biotin)·streptavidin was synthesized as described.[6] The fluorogenic substrates (Leu-Arg-Gly-Gly-$NH)_2$-rhodamine and (Cbz-Leu-Arg-Gly-Gly-$NH)_2$-rhodamine were synthesized and purified as described previously (26, 37). AVP and the AVP mutant C122A[7] were purified using published procedures (26, 34). Coomassie Blue-stained or silver-stained protein gels were scanned on a flatbed scanner, and the bands were quantitated with the GE Healthcare ImageQuant software. Buffer A was 20 mM Hepes (pH 7.0), 0.025% (w/v) DDM, and 0.1 mM DTT. Buffer B was 20 mM Tris-HCl (pH 8.0), 0.025% DDM, and 0.1 mM DTT. pVIc was labeled with Cy3B as described previously.[6]

Cloning of pVI and VI—Expression plasmids containing the pVI or VI open reading frames were acquired in two steps. First, PCR products were synthesized using Ad2 genomic DNA (Sigma) as template. The pVI ORF PCR product was inserted between a BsaI site and a blunt end. The VI ORF PCR product was inserted between NdeI and BamHI sites. Primers were purchased from Invitrogen. Sequences of the primers were as follows: for pVI, the forward primer, pVIf, was 5′-AAG GGT CTC ACA TGG AAG ACA TCA ACT TTG CGT CTC TG-3′ and incorporated a BsaI site (underlined). The reverse primer, pVIr, was 5′-GAA GCA TCG TCG GCG CTT CAG GGA TTG-3′ with a blunt end. For VI, the forward primer, VIf, was 5′-ATT CCA TAT GGC CTT CAG CTG GGG CTC GCT G-3′ and incorporated an NdeI site (underlined), and the reverse primer, VIr, 5′-GGT TGG ATC CTT ACA GAC CCA CGA TGC TGT TCA G-3′ incorporated a BamHI site (underlined). For efficient VI expression, VIf contained an initiator Met codon just prior to the Ala codon at the site of the N-terminal consensus cleavage site of the adenovirus proteinase, and VIr contained a stop codon after the Leu codon at the consensus cleavage site of the adenovirus proteinase near the C terminus of pVI. After restriction, protein VI was ligated into a pET13a vector, whereas pVI was ligated into a pREX-S31 vector. The resultant plasmids were subcloned into Top10 cells. Sequence verification was performed to ensure the presence of the correct reading frame and absence of mutations. pVI- and VI-expressing bacteria were obtained by transformation of *E. coli* BL21 (DE3) RIL Codon Plus cells for both constructs.

Expression of pVI and VI—The genes for pVI and VI were expressed overnight at 37 °C by autoinduction in ZYM-5052 medium (38). The bacterial cells were collected by centrifugation at 20,000 × *g* for 20 min and stored at −20 °C. Protein expression was confirmed by SDS-PAGE on bacterial lysates.

Purification of pVI and VI—Frozen *E. coli* cell paste (~5 g) was suspended in 50 ml of lysis buffer containing 50 mM Tris-

[5] The following designations are used in this study: AVP-pVIc, noncovalent or covalently linked heterodimer of AVP and pVIc; pVIc, 11-amino acid cofactor (GVQSLKRRRCF) originating from the C-terminus of virion precursor protein pVI.

[6] P. C. Blainey, V. Graziano, W. J. McGrath, G. Luo, X. S. Xie, and W. F. Mangel, submitted.

[7] W. J. McGrath and W. F. Mangel, unpublished observations.

HCl (pH 7.5), 100 mM NaCl, 5 mM EDTA, 1% DDM, 1 mM DTT, 1 mM PMSF, 1 mM benzamidine-HCl, and 1 tablet of Complete, EDTA-free protease inhibitor mixture (Roche Applied Science). Lysozyme to 0.01 mg/ml was added, and the cell suspension was mixed by end-over-end rotation at room temperature for 60 min. The cell lysate was then sonicated intermittently for 5 min on ice. Nucleic acids were further digested by the addition of 2.5 units of Benzonase. The suspension was clarified by centrifugation at 10 °C in an SS-34 rotor for 30 min at 30,000 × *g*. The supernatant was diluted 2-fold to lower the salt concentration and with a peristaltic pump loaded onto a low pressure 40-ml Macro-Prep high S cation-exchange cartridge. The cartridge had previously been equilibrated in 25 mM MES (pH 6.5), 0.1 mM EDTA, 1 mM DTT, and 0.05% DDM. The flow rate was 3 ml/min. Proteins were eluted using 15 column volumes of a linear salt gradient between 0 and 1 M NaCl. Protein elution was monitored at 280 nm, and 1-min fractions were collected. Fractions containing pVI were identified by SDS-PAGE on a 15% polyacrylamide gel and pooled; protein in the pool was concentrated in an Amicon Ultra 10,000 molecular weight cut-off membrane. The pVI was then diluted 3-fold with 25 mM MES (pH 6.5), 0.1 mM EDTA, 1 mM DTT, and 0.05% DDM and loaded onto a 15-ml POROS 20 HS cation-exchange column at a flow rate of 2 ml/min. Proteins were eluted in a 20 column volume linear gradient from 0 to 500 mM NaCl. Fractions containing pVI were identified by SDS-PAGE and pooled; the pVI was concentrated to about 1 ml. pVI was further purified by size-exclusion chromatography on a HiLoad 16/60 Superdex 200 prep grade column (Amersham Biosciences). The column was equilibrated with 25 mM Tris-HCl (pH 7.5), 150 mM NaCl, 0.1 mM EDTA, 1 mM DTT, and 0.05% DDM. The flow rate was 0.75 ml/min; 1 ml of sample was injected. The protein elution profile was obtained from the optical density at 280 nm, and 2-min fractions were collected. Fractions with pVI greater than 98% pure were identified by SDS-PAGE and pooled. The pooled fractions were diluted 5-fold with 25 mM MES (pH 6.5), 0.025% DDM, 0.1 mM EDTA, and 1 mM DTT and then loaded onto a small cation-exchange column. The column was washed extensively, and the pVI was eluted with 0.8 M NaCl, 25 mM MES (pH 6.5), 0.1 mM EDTA, 0.025% DDM, and 1 mM DTT. This step not only led to pVI being more concentrated but also ensured that the concentration of DDM in the buffer was 0.025%. Fractions with pure pVI were then dialyzed against storage buffer, which contained 12.5 mM MES (pH 6.5), 0.025% DDM, 25 mM NaCl, 0.1 mM EDTA, and 1 mM DTT. The concentration of pVI was determined using a calculated molar extinction coefficient of 30480 M^{-1} cm^{-1}. Aliquots of pVI were frozen in liquid nitrogen and stored at −80 °C. Protein VI was purified by the same procedure.

Equilibrium Dissociation Constants—Equilibrium dissociation constants from anisotropy experiments and enzymatic activity assays were calculated as described previously (32).

Purification of Hexon—Hexon was purified by modifications of the procedures of Burnett (39). CsCl top fractions from a crude extract of Ad2-infected HeLaS3 cells were thawed and dialyzed overnight against 1 liter of 10 mM Tris-HCl, pH 8, at 4 °C. After dialysis, the solution was centrifuged for 30 min at 4 °C at 6700 × *g* to remove any insoluble material. All further chromatography steps were carried out at 21 °C. The clarified solution was loaded onto a 15-ml Fractogel EMD TMAE Hicap (M) strong anion-exchange column at a flow rate of 2 ml/min. The column was washed extensively with 10 mM Bis-Tris-propane, pH 7, and bound proteins were eluted with a linear salt gradient from 0 mM to 500 mM NaCl. Hexon-enriched fractions were identified by SDS-PAGE and eluted from the column around 0.4 M NaCl. The fractions were pooled (~20 ml), diluted 1:2 with 10 mM Bis-Tris-propane, pH 7, and loaded onto a 15-ml POROS 20 HQ strong anion-exchange column, previously equilibrated in the same buffer. Hexon was eluted from the column with a linear salt gradient as described above except that it eluted at 0.65 M NaCl. Pure hexon fractions were identified by SDS-PAGE, pooled, and dialyzed against 1 liter of storage buffer consisting of 10 mM sodium phosphate, pH 7, 0.02% sodium azide. Hexon was quantitated spectrophotometrically using a calculated extinction coefficient of 156430 $M^{-1}cm^{-1}$ and stored on ice.

Steady-state Fluorescence Intensity and Anisotropy Measurements—Steady-state fluorescence intensity and anisotropy measurements were performed on an ISS PC-1 spectrofluorometer with 19-A lamp current, 564-nm excitation wavelength, and 580-nm emission filter. The G factor for anisotropy experiments was measured before the beginning of each experiment. 1 ml of Cy3B labeled pVI was placed inside a quartz cuvette in buffer containing 20 mM Hepes, pH 7, 150 mM NaCl. After each addition of hexon, the liquid was mixed by pipetting the solution up and down four times and allowed to reach equilibrium for 2 min before opening the shutters to acquire data. Steady-state fluorescence intensity data were acquired in the absence of polarizers to increase the fluorescence signal.

Photobleaching Data Analysis—Fluorescence images of an isolated and immobilized single molecule of (pVIc-biotin)·streptavidin-Alexa Fluor 546 complex or Cy3B-pVI were processed as follows. For each image frame, the average fluorescence peak intensity was calculated by summing all neighboring pixels with intensity values above a certain threshold and then dividing by the number of neighbors. All remaining pixels in that frame were considered background noise and were processed in a similar manner. The net peak intensity was obtained by subtracting the average background noise from the average peak intensity.

RESULTS

Cloning, Expression, and Purification of pVI and VI—The T7-based system (38) was employed for the cloning and expression of the adenovirus precursor protein pVI and its proteolytically processed, mature form, protein VI, as described under "Experimental Procedures." Purification of pVI and VI was accomplished by cation-exchange and size-exclusion chromatography. The proteins were about 99% pure, as assessed by SDS-PAGE (see Fig. 6*B*) and by MALDI-TOF analysis. pVI and VI required a detergent to keep them in solution. Below a concentration of DDM of 0.0125%, the proteins were insoluble, as determined by dynamic light scattering.

Binding of pVI and Protein VI to DNA—The interactions of pVI and VI with DNA have not been previously characterized. We used fluorescence anisotropy to measure the $K_{d(app)}$ for the binding of pVI to dsDNA. Aliquots of pVI were added to a solution of 33-mer dsDNA in which one of the strands was labeled at its 5′-end with fluorescein, and the fluorescence ani-

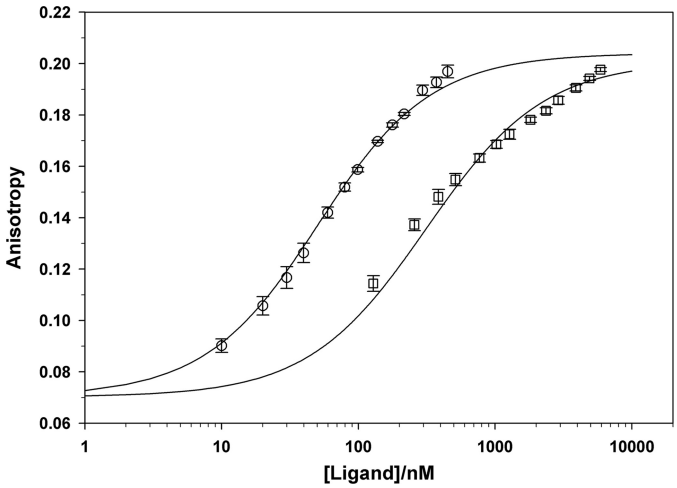

FIGURE 1. **Binding of pVI and VI to DNA.** Equilibrium dissociation constants were calculated. Aliquots of pVI or VI were added to buffer B with 1 mM $MgCl_2$ containing 10 nM fluorescein-labeled 33-mer dsDNA, and the steady-state anisotropy after each addition was measured at 21 °C. The data are presented in the form of a Bjerrum plot and yielded apparent equilibrium dissociation constants of 46 ± 1.6 nM for pVI (*open circles*) and 307 ± 38 nM for VI (*open squares*). Data points are averages of three replicates ± S.D. The *solid lines* were obtained by inverse variance weighted nonlinear regression fit of a 1:1 ligand-receptor binding model to the data.

sotropy was determined as described under "Experimental Procedures." The data are presented in Fig. 1 in the form of a Bjerrum plot. The $K_{d(app)}$ was 46 ± 1.6 nM (Table 1). A similar experiment was performed with protein VI (Fig. 1). The $K_{d(app)}$ was much higher, 307 ± 38 nM (Table 1). These binding assays were done in 1 mM $MgCl_2$ because in the absence of magnesium, the binding to DNA was too tight to determine a $K_{d(app)}$.

Stoichiometry of Binding of pVI to DNA—How many molecules of pVI bind to one molecule of 60-mer dsDNA? The stoichiometry of binding of pVI to DNA was ascertained using fluorescence anisotropy under tight binding conditions, conditions in which the concentration of one of the ligands was at least 10-fold greater than its $K_{d(app)}$. Increasing amounts of pVI were added to a constant amount of 5′-fluorescein-labeled 60-mer dsDNA, and the change in anisotropy upon each addition was measured. The concentration of fluorescein-labeled dsDNA was much higher than the $K_{d(app)}$. Under these tight binding conditions, at pVI concentrations below saturation of DNA, all pVI present will be bound to DNA; above saturation, no added pVI will be able to bind to DNA. As shown in Fig. 2*A*, as the concentration of pVI was increased, the anisotropy increased linearly. Once saturation was reached, there was no further increase in anisotropy as additional pVI was added. The data points could be characterized by two straight lines using a linear fitting routine. The intersection point of the two lines is the minimal concentration of pVI required to saturate the DNA. Because this occurred at a concentration of pVI of 110 nM and the concentration of 60-mer dsDNA was 13.7 nM, the stoichiometry of binding of pVI to 60-mer dsDNA was 8:1, eight molecules of pVI per molecule of 60-mer dsDNA. Similar experiments were performed with 33-mer, 18-mer, and 12-mer dsDNA.[8] When the maximal number of molecules of pVI bound to one DNA molecule is plotted *versus* the DNA length in base pairs, a straight line through the origin was observed (Fig. 2*B*). This implied that one molecule of pVI occluded 8 bp of DNA. Most important, these data also indicated that pVI bound to DNA independent of the sequence of the DNA.

Number of Ion Pairs in the Binding of pVI to DNA—To further characterize the DNA binding interface, we determined the number of ion pairs involved in the binding of pVI to DNA. At different ionic strengths, 12-mer dsDNA labeled at one of its 5′ ends with fluorescein was incubated with increasing concentrations of pVI. The equilibrium dissociation constants (K_d) were determined by fluorescence anisotropy (Fig. 3*A*). The log (K_d) was plotted *versus* log[NaCl] (Fig. 3*B*). The following equation describes the resultant straight line

$$-\frac{\partial \log K_d}{\partial \log (M^+)} = m'\psi \qquad \text{(Eq. 1)}$$

where M+ is the monovalent counterion concentration, m' is the number of ion pairs formed, and ψ is the fraction of a counterion associated, in the thermodynamic sense, with each phosphate of DNA in solution. For dsDNA, ψ is 0.88 (40). The number of ion pairs formed upon binding of a pVI to 12-mer dsDNA was 2.9.

Nonelectrostatic Free Energy of Binding of pVI to dsDNA—The nonelectrostatic change in free energy, ΔG_0^0, upon binding of pVI to DNA was also calculated. The line in Fig. 3*B* was extrapolated to a Na^+ concentration of 1 M. Then, the following equation was used

$$\Delta G_0^0 = -RT\ln K_o \qquad \text{(Eq. 2)}$$

where K_o is K_A in 1 M Na^+. The ΔG_0^0 (1 M Na^+) was −4.0 kcal/mol. By correction for three lysine-like ion pairs, which have a ΔG_0^0 (1 M Na^+) of 3 × 0.18 kcal, the nonelectrostatic free energy of binding was calculated to be −4.54 kcal/mol. The K_d values from Fig. 3*A* were 60, 144, 327, 452, and 1036 nM in 0.02, 0.03, 0.04, 0.05, and 0.06 M NaCl, respectively. By extrapolation of the line (Fig. 3*B*), the K_d in 1 M NaCl was 1154 μM.

pVI Slides Along DNA as a Monomer—The oligomeric state of pVI was difficult to determine because pVI requires detergent to be soluble. For this reason, we resorted to an indirect assay, a single-molecule photobleaching assay, to see whether pVI is a monomer or an oligomer.

In the image series of pVI sliding along DNA, occasionally a labeled molecule of pVI would be seen to stick irreversibly to the glass surface of the coverslip (41). If the exciting light remained on, eventually the fluorophore would bleach. Such an event, with labeled pVI from a pVI preparation that had a ratio of Cy3B label to protein of 0.9, is shown in Fig. 4*A*. Before the Cy3B-labeled molecule of pVI stuck to a spot on the glass, the fluorescence intensity at that spot was zero. Upon pVI sticking to the glass, the fluorescence intensity abruptly increased. The fluorescence intensity remained constant for about 0.5 s and then abruptly decreased to zero. Abrupt, one-step photo bleaching of a molecule irreversibly bound to the glass slide is characteristic of the visualization of a protein molecule labeled with a single dye molecule. Were the fluorescence from more than one dye molecule on a protein or from more than one labeled protein, upon bleaching, the fluorescence would have

[8] V. Graziano and W. F. Mangel, unpublished observations.

TABLE 1
Binding to DNA and sliding along DNAs via one-dimensional diffusion of adenovirus proteins

Species and molecular weight	Ligand for $K_{d(app)}$ analysis	$K_{d(app)}$[a]	DNA binding site (length)	One-dimensional diffusion constant[b]
		nM	*bp*	$(bp)^2/s \times 10^{-6}$
pVI 27,014	33-mer dsDNA	46 ± 1.6	8	1.45 ± 0.13[c]
pVI 27,014	Hexon	1.1 ± 0.16		
VI 22,118	33-mer dsDNA	307 ± 38		
pVIc[d] 1350	12-mer dsDNA	264 ± 25		26.0 ± 1.8
AVP[e] 23087	12-mer dsDNA	63 ± 5.8		
AVP-pVIc 24435	36-mer dsDNA	4.6 ± 2.2[e]	6[e]	21.0 ± 1.9[f]

[a] The error in $K_{d(app)}$ denotes the standard error obtained from inverse variance weighted nonlinear regression fit of the data.
[b] To convert from bp to nm: 10^6 $(bp)^2/s$ = 102,400 $(nm)^2/s$.
[c] Ref. 41.
[d] Footnote 6.
[e] Ref. 32.
[f] Ref. 42.

diminished in multiple steps as several colocalized dye molecules would not likely bleach simultaneously. One-step photo bleaching was observed in 30 out of 30 bleaching events. Because in the same microscope field the fluorescence intensities of the molecules that were sliding on DNA were the same as those that stuck to the glass whose bleaching was observed, we conclude that under these conditions, pVI was sliding along DNA as a monomer. In a control experiment (Fig. 4*B*), a (pVIc-biotin)·streptavidin complex[6] with two molecules of Alexa Fluor 546 per streptavidin molecule irreversibly stuck to the glass surface during a sliding assay. Although its fluorescence intensity rose abruptly upon binding to the glass surface, bleaching occurred in two steps, as predicted from the labeling quantization.

pVI Binding to Hexon—The interactions of purified pVI to the hexon trimer have not been quantitatively characterized. We used fluorescence quenching to measure the $K_{d(app)}$ for the binding of pVI to hexon. Aliquots of hexon were added to a solution of pVI labeled with Cy3B, and the intensity of fluorescence was determined as described under "Experimental Procedures." The data are presented in Fig. 5*A*. The $K_{d(app)}$ was 1.1 ± 0.16 nM (Table 1).

Stoichiometry of Binding of pVI to Hexon—How many molecules of pVI bind to one molecule of hexon? The stoichiometry of binding of pVI to hexon was ascertained using fluorescence anisotropy under tight binding conditions. In this case, the concentration of Cy3B-labeled pVI, 20 nM, was more than 10-fold greater than its $K_{d(app)}$ for binding to hexon. Experimentally, increasing amounts of hexon were added to a constant amount of Cy3b-labed pVI, and the change in anisotropy upon each addition was measured. As shown in Fig. 5*B*, as the concentration of hexon was increased, the anisotropy increased linearly. Once saturation was reached, there was no further increase in anisotropy as additional hexon was added. The data points could be characterized by two straight lines using a linear fitting routine. The intersection point of the two lines is the minimal concentration of hexon required to saturate pVI. Because this occurred at a concentration of hexon of 25 nM, and the concentration of pVI was 20 nM, the stoichiometry of binding of pVI to hexon monomer was 1:1.

The Form of Hexon to Which pVI Binds—In solution and in the crystal structure, hexon is a trimer. Our data showed that one molecule of pVI binds to one molecule of hexon. Does this mean that three molecules of pVI bind to one molecule of hexon trimer? Fig. 6 shows a chromatogram of hexon and hexon·pVI complexes from size-exclusion chromatography analysis. Although the estimated molecular weight of hexon is consistent with that of a trimer, an estimate of the molecular weight of the hexon·pVI complex is problematic because we do not know the overall shape of the complex. Given the large shift in retention time of the hexon·pVI complex, it is likely that pVI induces a rather large conformational change in the hexon structure.

DISCUSSION

The gene for pVI was cloned and expressed in *E. coli*, and the resultant protein was purified and characterized. pVI was purified to homogeneity. pVI had not been purified before, and some of the previous experiments with pVI and protein VI were done with proteins that had at one time been denatured (17). The binding of pVI to DNA was independent of DNA sequence and was very tight. The $K_{d(app)}$ for the binding of pVI to DNA was 46 nM. However, the binding assays had to be done in 1 mM $MgCl_2$ because in the absence of magnesium, the binding to DNA was too tight to determine a $K_{d(app)}$. A similar problem arose in characterizing the binding of pVI to hexon. At 10 nM, we observed tight binding; this implied that the $K_{d(app)}$ was probably much lower. The binding of pVI to DNA was mediated by ionic contacts as the binding was sensitive to ionic strength. On the other hand, the binding of pVI to hexon can occur even in the presence of 1 M NaCl. However, that binding appeared to be due to hydrophobic interactions as that interaction was sensitive to detergents.[8]

pVI is a monomer at nM concentrations. Previously, we had shown that pVI slides along DNA via one-dimensional diffusion (41); its one-dimensional diffusion constant is 1.45×10^6 bp/s. In the sliding assays, we observed photo bleaching of pVI. Because the drop in fluorescence due to bleaching occurred in a single step, we concluded that pVI was sliding as a monomer. Both pVI and VI required a detergent to be soluble. As judged by dynamic light scattering, the minimum amount of DDM required for pVI to remain in solution was 0.0125%.

pVI may bind to DNA mostly through its pVIc moiety. The $K_{d(app)}$ for the binding of pVI to DNA was 46 nM. AVP-pVIc complexes also bind tightly to DNA. The $K_{d(app)}$ is 4.6 nM. Both protein VI and AVP bind less tightly to DNA. Their $K_{d(app)}$ values are almost 10-fold higher, 307 and 63 nM, respectively. Secondly, the number of base pairs covered while bound to DNA is similar; pVI covers 8 bp, and AVP-pVIc complexes

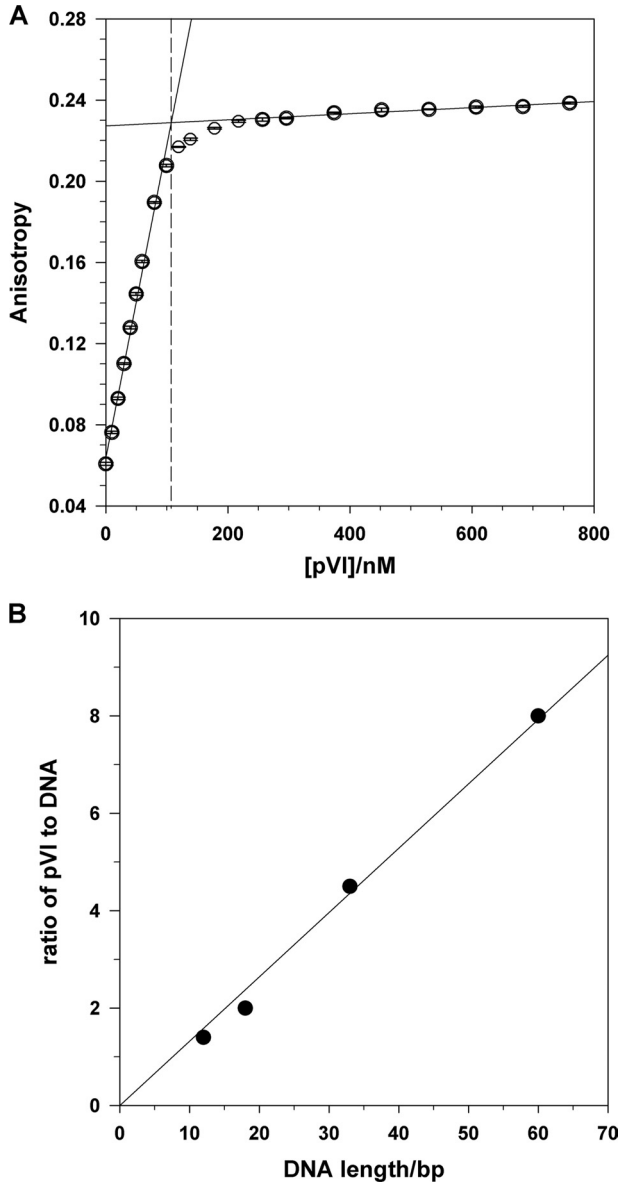

FIGURE 2. **Stoichiometry of binding of pVI to DNA.** *A*, stoichiometry of binding. Aliquots of pVI were added to solutions of buffer B containing 13.7 nM 60-bp DNA labeled at one 5′ end with fluorescein. After each addition, the steady-state anisotropy was measured. The *solid lines* are linear fits to the data. The point of intersection of the straight lines, the *dashed vertical line*, indicates that a minimum of 110 nM pVI was required to saturate 13.7 nM 60-bp dsDNA, a stoichiometry of binding of 8:1. The experiment was repeated with 33-mer, 18-mer, and 12-mer dsDNA.[8] Data points are averages of four replicates ± S.D. *B*, the number of base pairs occluded upon binding of pVI to DNA. The data from the experiments in *A* were used to plot the ratio of pVI to DNA *versus* DNA length (bp). The average number of bp per pVI binding site was 8.

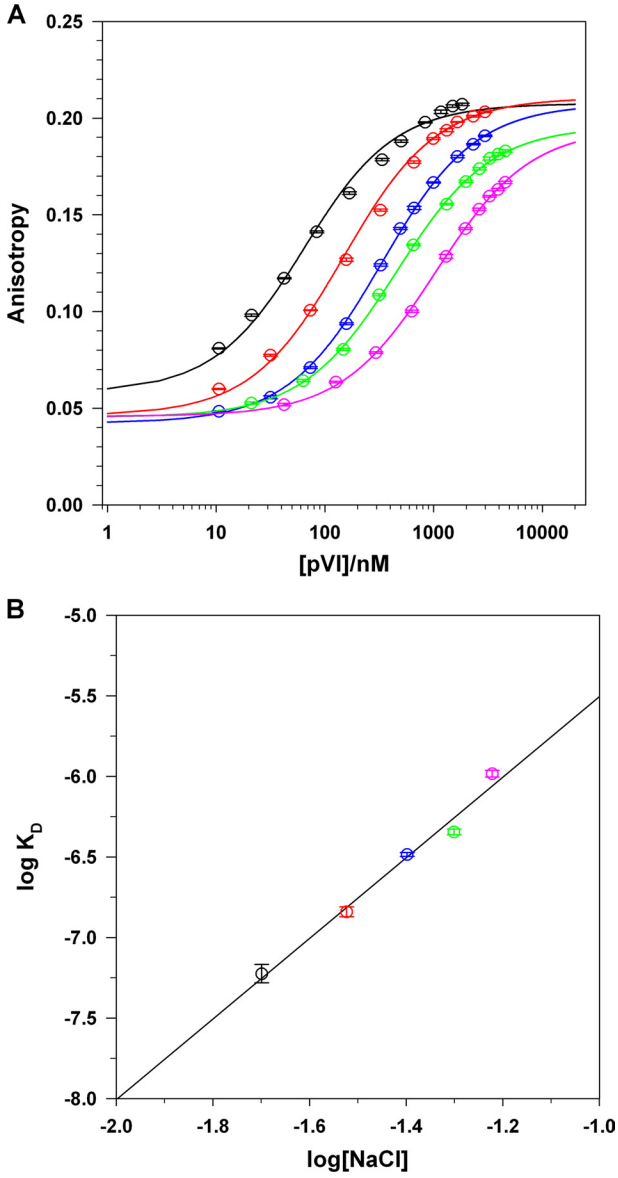

FIGURE 3. **Thermodynamic parameters in the binding of pVI to DNA.** *A*, number of ion pairs involved in binding of pVI to DNA. Binding isotherms of pVI binding to 10 nM fluorescein-labeled 12-mer dsDNA in buffer B are shown as a function of the NaCl concentration (*black*, 0.02 M; *red*, 0.03 M; *blue*, 0.04 M; *green*, 0.05 M; and *pink*, 0.06 M). Binding was measured by changes in fluorescence anisotropy as the pVI concentration was increased, as described under "Experimental Procedures." Data points are averages of four replicates ± S.D. The *solid curves* are inverse weighted nonlinear regression fit of the data to a 1:1 binding model. *B*, changes in nonelectrostatic free energy upon the binding of pVI to DNA. The log of the equilibrium dissociation constants calculated from the data in *A* are plotted *versus* −log [NaCl]. The *error bars* denote the S.E. in the K_d value obtained from the nonlinear regression fit of the data in *A*. The *solid line* is a weighted linear regression fit of the data.

cover 6 bp (32). In contrast, the virion precursor protein pIIIa covers 33 bp.[8] Third, some thermodynamics parameters of pVI binding to DNA are similar to those of AVP-pVIc complexes binding to DNA (32), namely the number of ion pairs formed and the nonelectrostatic free energy of binding.

The nonsequence-specific interaction between pVI and DNA exhibited a substantial dependence on monovalent sodium ion concentration. This dependence reflects the electrostatic component of the binding reaction (40). The electrostatic component originates from the formation of ion pairs between positively charged groups on pVI and negatively charged phosphate groups on DNA. After binding occurs, there is a concomitant release of counterions from the DNA and, possibly, from pVI. From an analysis of the equilibrium association constants for the binding of pVI to 12-mer dsDNA as a function of the Na^+ concentration, an accurate estimate of the number of ion pairs involved in the interaction was obtained. Three ion pairs were involved in binding to 12-mer dsDNA. For comparison, two ion pairs of AVP-pVIc complexes are involved in its interaction with DNA (32).

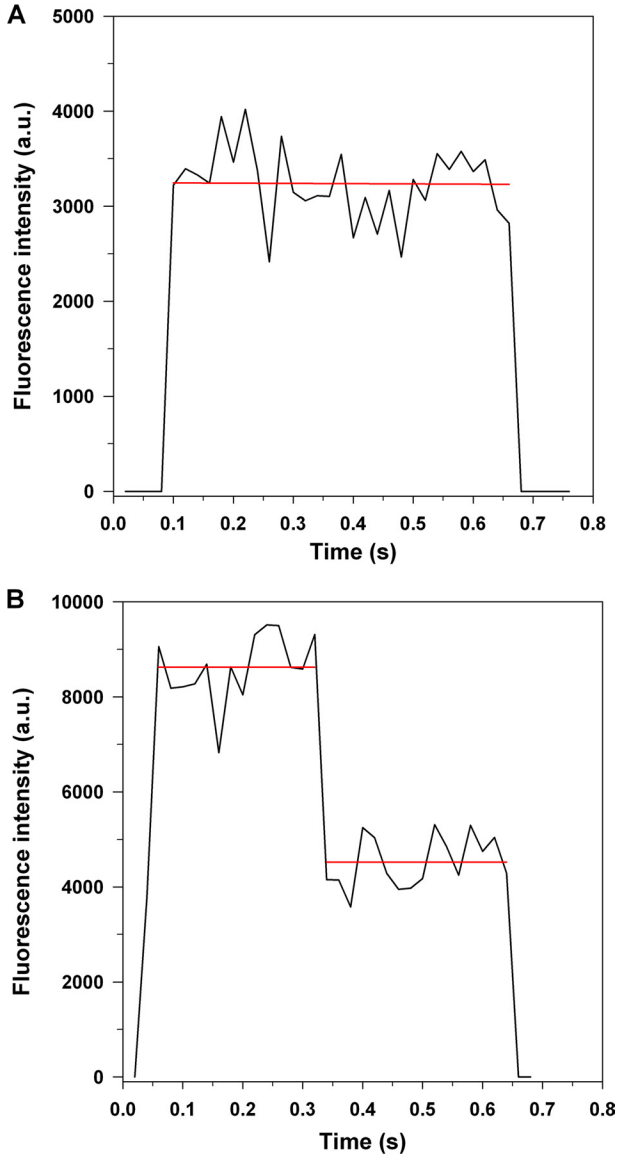

FIGURE 4. **Oligomeric state of pVI determined by single molecule photo bleaching.** *A*, in an image series (1.2 kW/cm^2, 0.00352 s/frame) of a sliding assay of pVI molecules labeled with Cy3B at an efficiency of 0.9 Cy3B molecules/pVI molecule, one of the molecules irreversibly stuck to a spot on the surface of the glass coverslip; the fluorescence intensity at that spot was recorded as a function of time. Bleaching occurred in one step. *a.u.*, arbitrary units. *B*, an experiment similar to that in *A* except that a molecule of a (pVIc-biotin)·streptavidin complex labeled with two molecules of Alexa Fluor 546[8] stuck to a spot on the surface of the glass coverslip. The bleaching of the (pVIc-biotin)·streptavidin complex occurred in two steps. The *red line* is the average intensity in that time range.

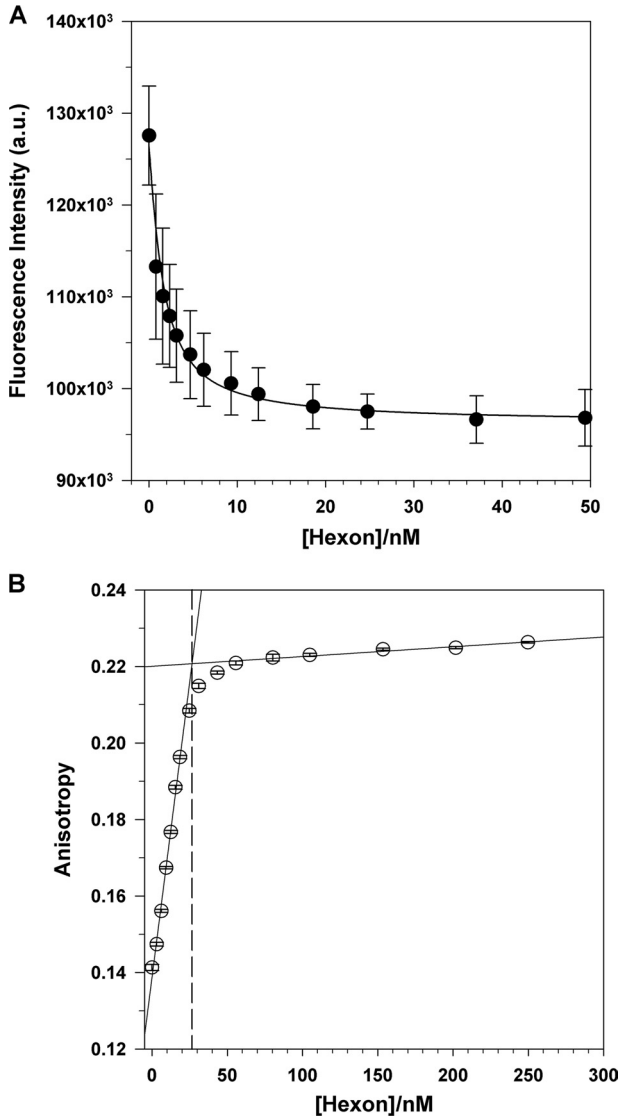

FIGURE 5. **Equilibrium binding and tight binding of pVI to hexon.** *A*, change in fluorescence intensity when 1 nM Cy3B-pVI is titrated with hexon in 20 mM Hepes, 150 mM NaCl, pH 7. Both pVI and hexon concentrations are reported as monomer concentrations. The dissociation constant (K_d) was determined by inverse variance weighted nonlinear regression fit of the steady-state fluorescence intensity data to a single site receptor-ligand binding model. The K_d is 1.1 ± 0.16 nM. Data points are averages of five replicates ± S.D. *B*, binding data for pVI-hexon interaction under tight binding condition. Changes in fluorescence anisotropy are observed when 20 nM of Cy3B-pVI is titrated with increasing amounts of hexon (monomer concentration) in buffer containing 20 mM Hepes, 150 mM NaCl, pH 7. The stoichiometry of binding is determined by the intersection of the two linear regression lines from the first seven and last six data points. Data points are averages of four replicates ± S.D.

There also seems to be a substantial, favorable nonelectrostatic component of the binding interaction. Upon extrapolation to 1 M Na^+ of the line in Fig. 3*B*, the ΔG_0^0 was −4.0 kcal/mol for pVI. The ΔG_0^0 is −4.2 kcal/mol for AVP-pVIc complexes (32). Correction for three lysine-like ion pairs makes the nonelectrostatic free energy of binding −4.5 kcal/mol for pVI. This indicates that a substantial component of the binding free energy under physiological conditions results from nonspecific interactions between pVI and base or sugar residues on the DNA and that the dominant factor driving the nonspecific interaction between pVI and DNA is the entropic contribution from the release of counterions.

Although it had been known that pVI binds to hexon (17), pVI had not, heretofore, been purified so that its interaction with hexon could be quantitatively characterized. In the virion, hexon appears as a homotrimer and is the major component of the capsid, forming the faces of the icosahedral surface. The arrangement of the hexon trimers alters at the vertices of the capsid, where the peripentonal hexons interact with the penton base. Our data on the binding of pVI to hexon showed that one molecule of pVI binds to one hexon molecule. Perhaps after pVI escorts hexon into the nucleus, some pVI dissociates from hexon and binds to the viral DNA because the local viral DNA

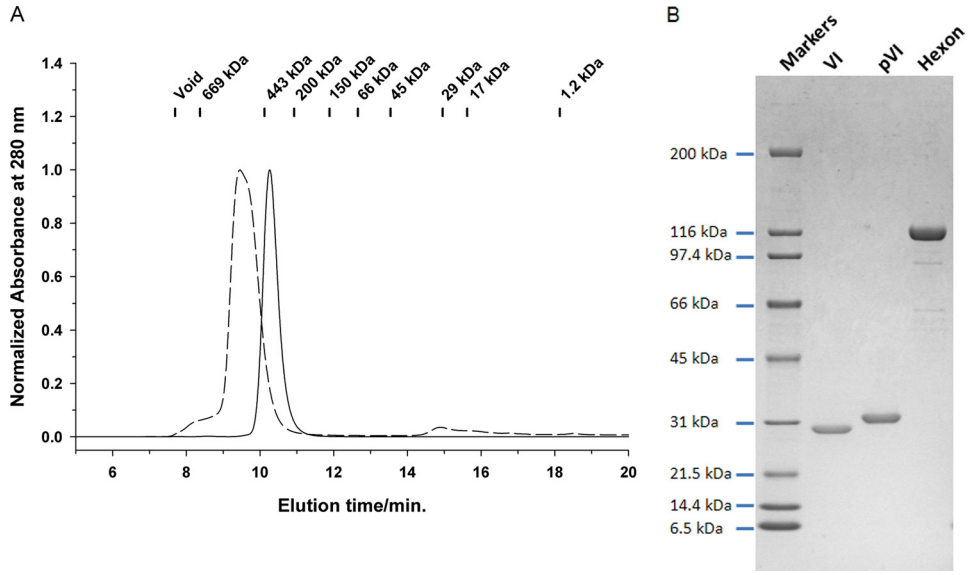

FIGURE 6. **Size-exclusion chromatography of hexon·pVI complexes.** *A*, gel filtrations of hexon and hexon·pVI complexes. The samples were injected onto a 7.8 mm × 30-cm TSK-GEL G3000SWXL analytical size-exclusion column and eluted with 25 mM MES, pH 6.5, containing 250 mM NaCl. The *vertical marks* on the *top* correspond to elution times of known molecular weight standards, with their molecular masses shown on top. The apparent molecular weights of Ad2 hexon and Ad2 hexon·pVI were determined by interpolation from the standard curve. *Solid line*, Ad2 hexon; *dashed line*, Ad2 hexon·pVI complex. *B*, SDS-polyacrylamide gel electrophoresis of purified proteins VI, pVI, and hexon (*lanes 2–4*). *Lane 1* contains molecular weight markers, with their molecular masses shown on the *far left*. The proteins were run on a 4–20% polyacrylamide gradient gel and stained with Coomassie Blue.

concentration is so high. After virion assembly, pVI then activates AVP on the DNA, and the resultant protein VI, given its 10-fold higher $K_{d(\mathrm{app})}$, dissociates from the DNA and binds to its final position in infectious virus.

There are multiple functions at the two ends of pVI. pVI is processed by AVP first at its N terminus and then at its C terminus (41). Upon processing by AVP, some of these functions may be terminated and others derepressed. The N terminus of pVI has membrane lytic activity (5). Initially, AVP cleaves off a peptide from pVI that contains amino acids 1–33. This may expose a predicted amphipathic α-helix (residues 36–53) that has been shown to be essential for membrane lytic activity in protein VI. Alternatively, the membrane lytic activity at the N terminus of pVI may be buried within hexon and exposed only after pVI dissociates from hexon. The last 11 amino acids of pVI, amino acids 239–250, facilitate binding to DNA. Their removal is reflected in the almost 10-fold higher $K_{d(\mathrm{app})}$ for protein VI relative to that of pVI. Also, the removed C-terminal peptide, pVIc, activates AVP (26, 27) and enables it to slide along DNA via one-dimensional diffusion to process the virion precursor proteins (42). Premature exposure of the membrane lytic activity before virion assembly or premature activation of AVP may be harmful to the infected cell, inhibit virion assembly, and possibly abort the infection. For example, if pVIc is added to cells along with adenovirus, the yield of infectious virus is down by more than 99% (35).

pVI and its processed form protein VI are remarkable proteins because they exhibit many quite different functions at various stages of an adenovirus infection. Two of those functions, binding to DNA and sliding along DNA, require nonspecific binding to DNA, which we have characterized here. Also, pVI binds tightly to hexon so that they can enter the nucleus together. It will be interesting to see how during virion assembly pVI dissociates from being tightly bound to hexon and binds tightly to the viral DNA, a prerequisite to the activation of AVP.

Acknowledgments—We thank Eileen Kasmarcik in the F. William Studier laboratory for cloning pVI and pIIIa and Michelle Louie for cloning protein VI.

REFERENCES

1. Greber, U. F., Willetts, M., Webster, P., and Helenius, A. (1993) Stepwise dismantling of adenovirus 2 during entry into cells. *Cell* **75,** 477–486
2. Strunze, S., Engelke, M. F., Wang, I. H., Puntener, D., Boucke, K., Schleich, S., Way, M., Schoenenberger, P., Burckhardt, C. J., and Greber, U. F. (2011) Kinesin-1-mediated capsid disassembly and disruption of the nuclear pore complex promote virus infection. *Cell Host Microbe* **10,** 210–223
3. Burckhardt, C. J., Suomalainen, M., Schoenenberger, P., Boucke, K., Hemmi, S., and Greber, U. F. (2011) Drifting motions of the adenovirus receptor CAR and immobile integrins initiate virus uncoating and membrane lytic protein exposure. *Cell Host Microbe* **10,** 105–117
4. Puntener, D., Engelke, M. F., Ruzsics, Z., Strunze, S., Wilhelm, C., and Greber, U. F. (2011) Stepwise loss of fluorescent core protein V from human adenovirus during entry into cells. *J. Virol.* **85,** 481–496
5. Wiethoff, C. M., Wodrich, H., Gerace, L., and Nemerow, G. R. (2005) Adenovirus protein VI mediates membrane disruption following capsid disassembly. *J. Virol.* **79,** 1992–2000
6. Moyer, C. L., Wiethoff, C. M., Maier, O., Smith, J. G., and Nemerow, G. R. (2011) Functional genetic and biophysical analyses of membrane disruption by human adenovirus. *J. Virol.* **85,** 2631–2641
7. Wodrich, H., Guan, T., Cingolani, G., Von Seggern, D., Nemerow, G., and Gerace, L. (2003) Switch from capsid protein import to adenovirus assembly by cleavage of nuclear transport signals. *EMBO J.* **22,** 6245–66255
8. Honkavuori, K. S., Pollard, B. D., Rodriguez, M. S., Hay, R. T., and Kemp, G. D. (2004) Dual role of the adenovirus pVI C terminus as a nuclear localization signal and activator of the viral protease. *J. Gen Virol* **85,** 3367–3376
9. Russell, W. C. (2009) Adenoviruses: update on structure and function. *J. Gen. Virol.* **90,** 1–20
10. Philipson, L. (1995) Adenovirus–an eternal archetype. *Curr. Top. Micro-*

biol. Immunol. **199,** 1–24
11. Liu, H., Jin, L., Koh, S. B., Atanasov, I., Schein, S., Wu, L., and Zhou, Z. H. (2010) Atomic structure of human adenovirus by cryo-EM reveals interactions among protein networks. *Science* **329,** 1038–1043
12. Saban, S. D., Silvestry, M., Nemerow, G. R., and Stewart, P. L. (2006) Visualization of α-helices in a 6-angstrom resolution cryoelectron microscopy structure of adenovirus allows refinement of capsid protein assignments. *J. Virol.* **80,** 12049–12059
13. Silvestry, M., Lindert, S., Smith, J. G., Maier, O., Wiethoff, C. M., Nemerow, G. R., and Stewart, P. L. (2009) Cryo-electron microscopy structure of adenovirus type 2 temperature-sensitive mutant 1 reveals insight into the cell entry defect. *J. Virol.* **83,** 7375–7383
14. Stewart, P. L., Fuller, S. D., and Burnett, R. M. (1993) Difference imaging of adenovirus: bridging the resolution gap between X-ray crystallography and electron microscopy. *EMBO J.* **12,** 2589–2599
15. van Oostrum, J., and Burnett, R. M. (1985) Molecular composition of the adenovirus type 2 virion. *J. Virol.* **56,** 439–448
16. San Martín, C., Glasgow, J. N., Borovjagin, A., Beatty, M. S., Kashentseva, E. A., Curiel, D. T., Marabini, R., and Dmitriev, I. P. (2008) Localization of the N-terminus of minor coat protein IIIa in the adenovirus capsid. *J. Mol. Biol.* **383,** 923–934
17. Russell, W. C., and Precious, B. (1982) Nucleic acid-binding properties of adenovirus structural polypeptides. *J. Gen. Virol.* **63,** 69–79
18. Bergelson, J. M., Cunningham, J. A., Droguett, G., Kurt-Jones, E. A., Krithivas, A., Hong, J. S., Horwitz, M. S., Crowell, R. L., and Finberg, R. W. (1997) Isolation of a common receptor for Coxsackie B viruses and adenoviruses 2 and 5. *Science* **275,** 1320–1323
19. Tomko, R. P., Xu, R., and Philipson, L. (1997) HCAR and MCAR: the human and mouse cellular receptors for subgroup C adenoviruses and group B coxsackieviruses. *Proc. Natl. Acad. Sci. U.S.A.* **94,** 3352–3356
20. Freimuth, P., Philipson, L., and Carson, S. D. (2008) The coxsackievirus and adenovirus receptor. *Curr. Top Microbiol. Immunol.* **323,** 67–87
21. Meier, O., Boucke, K., Hammer, S. V., Keller, S., Stidwill, R. P., Hemmi, S., and Greber, U. F. (2002) Adenovirus triggers macropinocytosis and endosomal leakage together with its clathrin-mediated uptake. *J. Cell Biol.* **158,** 1119–1131
22. Gastaldelli, M., Imelli, N., Boucke, K., Amstutz, B., Meier, O., and Greber, U. F. (2008) Infectious adenovirus type 2 transport through early but not late endosomes. *Traffic* **9,** 2265–2278
23. Wang, K., Huang, S., Kapoor-Munshi, A., and Nemerow, G. (1998) Adenovirus internalization and infection require dynamin. *J. Virol.* **72,** 3455–3458
24. Wodrich, H., Henaff, D., Jammart, B., Segura-Morales, C., Seelmeir, S., Coux, O., Ruzsics, Z., Wiethoff, C. M., and Kremer, E. J. (2010) A capsid-encoded PPxY-motif facilitates adenovirus entry. *PLoS Pathog* **6,** e1000808
25. Akusjärvi, G., Aleström, P., Pettersson, M., Lager, M., Jörnvall, H., and Pettersson, U. (1984) The gene for the adenovirus 2 hexon polypeptide. *J. Biol. Chem.* **259,** 13976–13979
26. Mangel, W. F., McGrath, W. J., Toledo, D. L., and Anderson, C. W. (1993) Viral DNA and a viral peptide can act as cofactors of adenovirus virion proteinase activity. *Nature* **361,** 274–275
27. Webster, A., Hay, R. T., and Kemp, G. (1993) The adenovirus protease is activated by a virus-coded disulphide-linked peptide. *Cell* **72,** 97–104
28. Matthews, D. A., and Russell, W. C. (1994) Adenovirus protein-protein interactions: hexon and protein VI. *J. Gen. Virol.* **75,** 3365–3374
29. Matthews, D. A., and Russell, W. C. (1995) Adenovirus protein-protein interactions: molecular parameters governing the binding of protein VI to hexon and the activation of the adenovirus 23K protease. *J. Gen. Virol.* **76,** 1959–1969
30. Ding, J., McGrath, W. J., Sweet, R. M., and Mangel, W. F. (1996) Crystal structure of the human adenovirus proteinase with its 11 amino acid cofactor. *EMBO J.* **15,** 1778–1783
31. McGrath, W. J., Ding, J., Didwania, A., Sweet, R. M., and Mangel, W. F. (2003) Crystallographic structure at 1.6-Ä resolution of the human adenovirus proteinase in a covalent complex with its 11-amino-acid peptide cofactor: insights on a new fold. *Biochim. Biophys. Acta* **1648,** 1–11
32. McGrath, W. J., Baniecki, M. L., Li, C., McWhirter, S. M., Brown, M. T., Toledo, D. L., and Mangel, W. F. (2001) Human adenovirus proteinase: DNA binding and stimulation of proteinase activity by DNA. *Biochemistry* **40,** 13237–13245
33. Bajpayee, N. S., McGrath, W. J., and Mangel, W. F. (2005) Interaction of the adenovirus proteinase with protein cofactors with high negative charge densities. *Biochemistry* **44,** 8721–8729
34. Mangel, W. F., Toledo, D. L., Brown, M. T., Martin, J. H., and McGrath, W. J. (1996) Characterization of three components of human adenovirus proteinase activity in vitro. *J. Biol. Chem.* **271,** 536–543
35. Baniecki, M. L., McGrath, W. J., McWhirter, S. M., Li, C., Toledo, D. L., Pellicena, P., Barnard, D. L., Thorn, K. S., and Mangel, W. F. (2001) Interaction of the human adenovirus proteinase with its 11-amino acid cofactor pVIc. *Biochemistry* **40,** 12349–12356
36. Gupta, S., Mangel, W. F., McGrath, W. J., Perek, J. L., Lee, D. W., Takamoto, K., and Chance, M. R. (2004) DNA binding provides a molecular strap activating the adenovirus proteinase. *Mol. Cell. Proteomics* **3,** 950–959
37. McGrath, W. J., Abola, A. P., Toledo, D. L., Brown, M. T., and Mangel, W. F. (1996) Characterization of human adenovirus proteinase activity in disrupted virus particles. *Virology* **217,** 131–138
38. Studier, F. W. (2005) Protein production by auto-induction in high density shaking cultures. *Protein Expr. Purif.* **41,** 207–234
39. Rux, J., and Burnett, R. M. (2007) Large-scale purification and crystallization of adenovirus hexon. In: *Adenovirus Methods and Protocols, Ad Proteins and RNA, Lifecycle and Host Interactions, and Phyologenetics* (Wold, W. S. M., and Tollefson, A. E., eds), 2nd Ed., pp. 231–250, Humana Press Inc., Totowa, NY
40. Record, M. T., Jr., Lohman, M. L., and De Haseth, P. (1976) Ion effects on ligand-nucleic acid interactions. *J. Mol. Biol.* **107,** 145–158
41. Graziano, V., Luo, G. Blainey, P. C., Pérez-Berná, A. J., McGrath, W. J., Flint, S. J., San Martín, C., Xie, X. S., and Mangel, W. F. (2012) Regulation of a viral proteinase by a peptide and DNA in one-dimensional space. II. Adenovirus proteinase is activated in an unusual one-dimensional biochemical reaction. *J. Biol. Chem.* **287,** 2068–2080
42. Blainey, P. C., Graziano, V., Pérez-Berná, A. J., McGrath, W. J., Flint, S. J., San Martín, C., Xie, X. S., and Mangel. W. F. (2012) Regulation of a viral proteinase by a peptide and DNA in one-dimensional space. IV. Viral proteinase slides along DNA to locate and process its substrates. *J. Biol. Chem.* **287,** 2092–2102

Regulation of a Viral Proteinase by a Peptide and DNA in One-dimensional Space: I. BINDING TO DNA AND TO HEXON OF THE PRECURSOR TO PROTEIN VI, pVI, OF HUMAN ADENOVIRUS

Vito Graziano, William J. McGrath, Maarit Suomalainen, Urs F. Greber, Paul Freimuth, Paul C. Blainey, Guobin Luo, X. Sunney Xie and Walter F. Mangel

J. Biol. Chem. 2013, 288:2059-2067.
doi: 10.1074/jbc.M112.377150 originally published online October 7, 2012